Available online at www.sciencedirect.com
ScienceDirect
International Journal of Mass Spectrometry 263 (2007) 171–178
International Journal of Mass Spectrometry
www.elsevier.com/locate/ijms

Photodissociation of lanthanide metal cation complexes with cyclooctatetraene

A.C. Scott, N.R. Foster, G.A. Grieves, M.A. Duncan *

Department of Chemistry, University of Georgia, Athens, GA 30602-2556, USA

Received 7 December 2006; received in revised form 22 January 2007; accepted 22 January 2007
Available online 30 January 2007

Abstract

Lanthanide metal (Sm, Dy, Nd) cation complexes with 1,3,5,7-cyclooctatetraene (COT) are produced by laser vaporization in a pulsed nozzle cluster source. The clusters are mass-selected and photodissociated using the third harmonic of a Nd:YAG laser (355 nm). Samarium–COT complexes prefer to form $[Sm_n(COT)_n]^+$ stoichiometries and fragment extensively when more than one metal atom is present in the cluster. However, the fragmentation patterns indicate the possible presence of multiple decker sandwich structures. Dysprosium–COT and neodymium–COT complexes prefer $[M_n(COT)_{n+1}]^+$ ratios, probably due to their preference for the +3 oxidation state. This stoichiometry pattern indicates that these clusters produce sandwich and multiple decker sandwich structures. Throughout the spectra for Dy and Nd complexes, a commonly occurring fragment is $[M(C_5H_5)]^+$. Fragmentation of the COT ligand occurs either because of a strong interaction with the metal or because of photochemical decomposition. Presuming that C_5H_5 exists as the cyclopentadienyl anion, the Dy and Nd metals in these fragments exist in an unusual +2 oxidation state.

Keywords: Cluster; Organometallic ion; Photodissociation

1. Introduction

A remarkable array of new organometallic complexes have been produced in recent years, including many examples of sandwich or multiple-decker sandwich structures [1–42]. Some of the best-known condensed phase examples of sandwich complexes, ferrocene [2] and dibenzene chromium [3], have motivated gas phase studies where problems with interfering solvent effects can be avoided. Experimental and theoretical work has explored sandwich complexes with benzene [4–10], fullerenes [10–25], and polycyclic aromatic hydrocarbons (PAHs) [26–35] as the ligand species. Some of these systems, such as transition metal–benzene complexes [4–10], metal–fullerene complexes [10–25], metal–PAH complexes [26–35], metal–cyclooctatetraene (COT) complexes [36–41], and even metal–ferrocene complexes [42], have exhibited multiple decker sandwich forms. Photodissociation has been used to shed light on the structures of these complexes [4–7,23–25,27–30,41]. In the present work, we use these photodissociation measurements to investigate the structures and stabilities of lanthanide metal–COT complexes.

Metal sandwich complexes with COT have been produced previously in the condensed phase [1,43–51] and in the gas phase [10,36–41]. Streitwieser and Müller-Westerhoff discovered uranocene in 1968 [43]. Uranocene is structurally analogous to ferrocene, but it contains uranium sandwiched between two COT ligands. According to Hückel's rule, a planar aromatic molecule must have $4n + 2$ electrons ($n = 0, 1, 2$, etc.). The COT molecule is therefore anti-aromatic because it has eight (i.e., $4n$) π electrons. In uranocene, stability is achieved because uranium donates two electrons to each ligand producing aromatic COT di-anions. These negatively charged ligands then have a favorable Coulombic attraction for the U^{4+} ion. This ionic bonding motif even makes it possible to form double-decker sandwiches via conventional synthetic chemistry, and several such species have been isolated and characterized [1,46]. Exploring similar concepts in the gas phase, Kaya and coworkers investigated the possibility of extended stacking for lanthanide metals with COT [10,36–40]. The mass spectra observed in their experiments showed a pattern of peaks corresponding to $[M_n(COT)_{n+1}]^+$ (M = Ce, Nd, Eu, Ho, Yb) species, which they assigned to multiple decker sandwiches. Photoelectron spectroscopy of these complexes were consistent

* Corresponding author. Tel.: +1 706 542 1998; fax: +1 706 542 1234.
E-mail address: maduncan@uga.edu (M.A. Duncan).

1387-3806/$ – see front matter © 2007 Elsevier B.V. All rights reserved.
doi:10.1016/j.ijms.2007.01.012

with this proposal, but there has been no direct spectroscopic confirmation of these gas phase structures.

Molecular beam photodissociation studies have been performed previously by our group for a variety of metal cation–ligand systems such as $M_n^+(benzene)_m$ [4–7], $M_n^+(C_{60})_m$ [23–25], and $M_n^+(PAH)_m$ [25,27–30]. Most recently, studies have been performed on transition metal–COT clusters [41]. In those systems, clusters of the form $M^+(COT)_{1,2}$ (M = V, Fe, Ni, Ag) were produced prominently, suggesting the formation of sandwich structures. Many of these systems dissociated via decomposition of the COT ligand, producing stable metal–benzene ions. Additionally, photodissociation of the vanadium and iron mono–COT complexes produced $M^+(C_5H_5)$ fragment ions. In transition metal–ligand bonding, stability is achieved through a synergistic mix of covalent and ionic interactions, in which the orbitals of the metal are able to donate to or accept charge from the ligands. Molecules gaining 18 electrons through this interaction show an increased stability, as in ferrocene and dibenzene chromium. However, while this mechanism is applicable to transition metal systems, previous experimental [45,46] and theoretical studies [46–49] have shown that the chemistry of the lanthanide metals usually involves purely ionic interactions. In the present study, we use photodissociation of lanthanide complexes with the anti-aromatic COT ligands to investigate the possible decomposition products that may be formed and what they can reveal about lanthanide organometallic bonding.

2. Experimental

Clusters for these experiments are produced by laser vaporization in a pulsed nozzle source. The experimental apparatus has been described previously [4–7,23–25,27–30]. The samples for these experiments are solid rods of samarium, dysprosium or neodymium. Because COT is a liquid at room temperature with relatively high vapor pressure, its ambient vapor is added to the system through a reservoir on the line feeding the expansion/backing gas to the nozzle. Argon is used as a backing gas with a pressure of 40–60 psi. Laser vaporization of the metal is accomplished using the second or third harmonic (532 and 355 nm, respectively) of a pulsed Nd:YAG laser (Spectra Physics GCR-11). The laser is focused onto the sample rod with a 30 cm focal length lens. The metal–COT complexes grow by recombination in a gas channel extension to the rod holder that is 1–2 cm in length. This expansion is skimmed into a differentially pumped chamber containing a reflectron time-of-flight mass spectrometer. In this chamber, the neutral clusters are photoionized with 193 nm from an ArF excimer laser (Lambda Physik Compex).

Mass-selected photodissociation experiments take place in the same reflectron time-of-flight mass spectrometer using pulsed deflection plates which allow size selection of certain cluster masses. The operation of the instrument for these experiments has been described previously [4–7,23–25,27–30]. The time-of-flight through an initial drift tube section is used to size select the desired cluster, which is then excited with a pulsed Nd:YAG laser at 355 nm (Spectra Physics GCR-11) in the turning region of the reflectron field. The time-of-flight through the second drift tube section provides a mass spectrum of the selected parent ion and its photofragments, if any. The data are presented in a computer difference mode in which the dissociated fraction of the parent ion is plotted as a negative mass peak while its photofragments are plotted as positive peaks. Mass spectra are recorded with a digital oscilloscope (LeCroy) and transferred to a laboratory PC via an IEEE-488 interface.

Laser power and wavelength studies are employed to investigate the possibility of multiphoton processes and sequential fragmentation processes. The laser power required to photodissociate these molecules varies considerably with their size and stability. The highest laser power employed for any cluster represents the full intensity of the unfocused Nd:YAG laser harmonics (e.g., about 100 mJ in a 1.0 cm^2 spot size). This would be our limit of "extremely high power." "High power," as used below, indicates 50–100 mJ/cm^2, while "low power" refers to 1–10 mJ/cm^2. Because we use a fixed wavelength for photodissociation (355 nm) the absorption efficiency also varies widely depending on the (unknown) wavelength dependence of the ultraviolet spectrum of these ions. We find in general that relatively high laser powers are required to see these photodissociation events. This is likely due to weak absorption, but it may also be caused by strong bonding in some systems. However, because of this, we are limited in the range of power dependence that can be studied.

3. Results and discussion

Fig. 1 shows mass spectra for each of the samarium, dysprosium, and neodymium–COT systems, respectively, produced by photoionization of neutral complexes that grow in the cluster

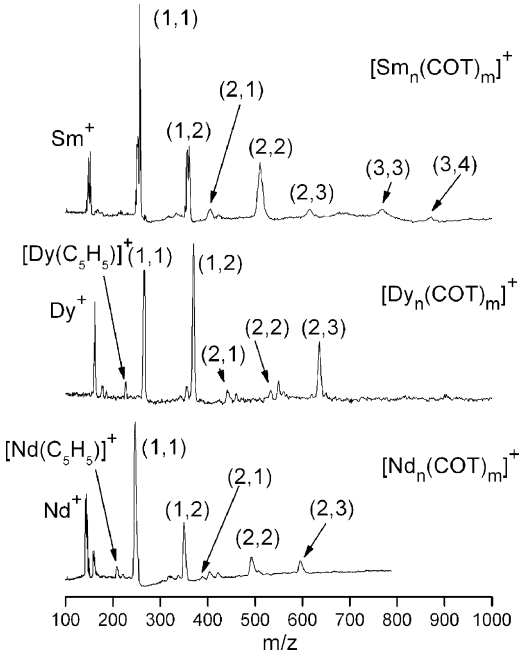

Fig. 1. These are the mass spectra of the complexes produced with the lanthanide metals samarium, dysprosium, and neodymium, respectively, with cyclooctatetraene.

source. It is important to note that the abundances in photoionization mass spectra such as these arise from several sources. Intense mass peaks can arise from abundant neutral clusters that ionize without extensive fragmentation, from clusters with low ionization thresholds that can be ionized with higher efficiency, or from the decomposition of larger clusters that produce stable cation fragments. It is therefore difficult to determine the source of these intensities. The ionization potential (IP) of COT (8.0 eV) [52] is relatively high, and we expect that at least some of these complexes may have IP's higher than the single photon energy (6.42 eV) at the ArF wavelength. Kaya and coworkers measured ionization potentials for the $M(COT)_{1,2}$ complexes for M = Nd, Eu, Ho, Yb, and all of these were lower than the ArF photon energy [36]. However, there is no data yet on the ionization potentials of the samarium or dysprosium systems. Therefore, we expect that these intensities may be influenced to some degree by ionization potentials and/or stable cation fragmentation products. We would usually sample ions directly from the cluster source to identify stable charged species, but the yield of direct ions was too small for this experiment. Therefore, we must use caution in deriving too much information from the intensities in these mass spectra.

Although the relative intensities in the mass spectra may be biased, we can still use the kinds of peaks detected to draw some useful conclusions. In the samarium–COT mass spectra (top frame, Fig. 1), there is a strong peak for $[Sm(COT)]^+$ (i.e., 1,1) followed by a less intense one for $[Sm(COT)_2]^+$. After the $[Sm(COT)_2]^+$ peak, a new series of clusters begins, with each containing two samarium atoms. This series consists of a weak $[Sm_2(COT)]^+$ peak, a stronger $[Sm_2(COT)_2]^+$ peak, and a weak $[Sm_2(COT)_3]^+$ peak. Finally, there are two weak signals corresponding to $[Sm_3(COT)_3]^+$ and $[Sm_3(COT)_4]^+$, with the $[Sm_3(COT)_3]^+$ peak being slightly more intense. Noticeably absent from this spectrum are any peaks corresponding to pure samarium clusters. Cluster masses containing multiple metal atoms are present, but only when there is also one or more ligand species present in a complex. This suggests that the metal–ligand bonding here is more favorable than the metal–metal bonding. Likewise, there are no ligand-only clusters here, suggesting that the metal ions are binding the ligands together. It is also important to note that the ratios of metal and ligand are not random. The 2,2 peak is more intense than the 2,1 feature, and there are noticeable peaks at 3,3 and 3,4 but no masses corresponding to $[Sm_3(COT)]^+$ or $[Sm_3(COT)_2]^+$. Apparently, roughly equal amounts of metal and ligand are preferred. Additionally, the absence of $[Sm(COT)_3]^+$ or any larger cluster with only one metal atom suggests that one samarium atom prefers to bind to a maximum of two COT ligands.

Overall, the samarium–COT mass spectrum suggests that these systems prefer an (n, n) type stoichiometry over the (n, $n+1$) one usually observed for sandwiches and multiple-decker sandwiches. It is possible to rationalize this in light of the oxidation states known for samarium. Although most of the lanthanide metals exhibit only $a+3$ oxidation state, samarium can also have $a+2$ state in some compounds. As noted above, the COT ligand often achieves stabilities in metal complexes by accepting charge to become an aromatic di-anion. It is then easy to rationalize the stability of a neutral Sm(COT) species as arising from the charge transfer of two electrons from Sm to COT, creating a stable, neutral complex with strong ionic bonding, i.e., Sm^{2+}, COT^{2-}. This is consistent with the fact that samarium has been reported to prefer the +2 oxidation state in the synthetically prepared half-sandwich complex and also that samarium–COT complexes are reported to be polymeric [50]. However, it is also possible to rationalize the 1,1 complex as a stable *cation* that might have a low ionization energy or be produced as a stable fragment from larger complexes. If Sm takes on the usual +3 oxidation state expected for the lanthanide metals, then a stable configuration could also be found for the $[Sm^{3+}, COT^{2-}]^+$ complex with an ion pair configuration and one net charge.

In the dysprosium mass spectrum, found in the middle frame of Fig. 1, there are $[Dy(COT)]^+$ and $[Dy(COT)_2]^+$ peaks. However, the $[Dy(COT)_2]^+$ peak is slightly larger in intensity than $[Dy(COT)]^+$, which is in contrast to the intensities found in the samarium mass spectrum. Additionally, as the spectrum continues, there are $[Dy_2(COT)_2]^+$ and $[Dy_2(COT)_3]^+$ peaks, but the intensity of the $[Dy_2(COT)_3]^+$ species is much larger than that of $[Dy_2(COT)_2]^+$. This is also in contrast to the samarium spectrum above. The neodymium–COT mass spectrum, the bottom frame of Fig. 1, shows a large $[Nd(COT)]^+$ peak followed by a less intense $[Nd(COT)_2]^+$ peak. After these, the intensities dip sharply with an almost non-existent $[Nd_2(COT)]^+$ peak, followed by almost equal intensity peaks of $[Nd_2(COT)_2]^+$ and $[Nd_2(COT)_3]^+$. Additionally, we see a small peak in each of the dysprosium and neodymium spectra corresponding to $[Dy(C_5H_5)]^+$ and $[Nd(C_5H_5)]^+$. The clusters in the dysprosium–COT mass spectrum seem to indicate that an (n, $n+1$) type stoichiometry is preferred for this system. Again, this can be explained through the use of oxidation states. Dysprosium strongly prefers the +3 oxidation state. Remembering that COT prefers to assume a di-anion state and that the ions photodissociated were initially neutral species in the source, the most natural neutral molecule created by the interaction of Dy (+3) with COT (−2) would be the $[Dy_2(COT)_3]$ complex. In both the dysprosium and neodymium data there is evidence for small amounts of oxide clusters. This apparently comes from some partial oxidation on the sample rod surface. Interestingly, these oxides appears as satellite masses with the 2,1 and 2,2 dysprosium peaks and the 2,1 neodymium peak. These species are metal-rich (ligand deficient) compared to others seen here, and the oxygen apparently fills out the metal coordination.

The mass spectra here can be contrasted with those seen previously by Kaya and coworkers [10,36–40]. The previous work looked at $M_n(COT)_m$ ((M = Ce, Nd, Eu, Ho, Yb) species, and found a strong preference for $m = n+1$ stoichiometries, with n,m cluster sizes seen up to values of 4,5 and 5,6. Therefore, larger clusters were seen in that previous work, and the preference for the n, $n+1$ stoichiometries was much stronger than in our experiments. The only metal studied by both groups is Nd, and these general differences seem to apply to the data for that metal system. These differences can be attributed to variations in the cluster source design and the relative concentrations of metal versus ligands in the two experiments.

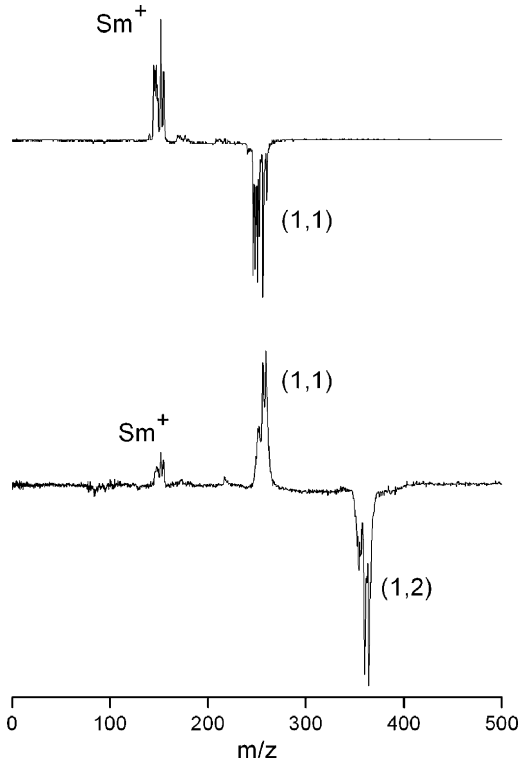

Fig. 2. The top frame shows the photodissociation spectrum of $[Sm(COT)]^+$ fragmented at 355 nm and at high laser power (defined in text). The lower frame shows the photodissociation spectrum of $[Sm(COT)_2]^+$ at 355 nm and at high laser power.

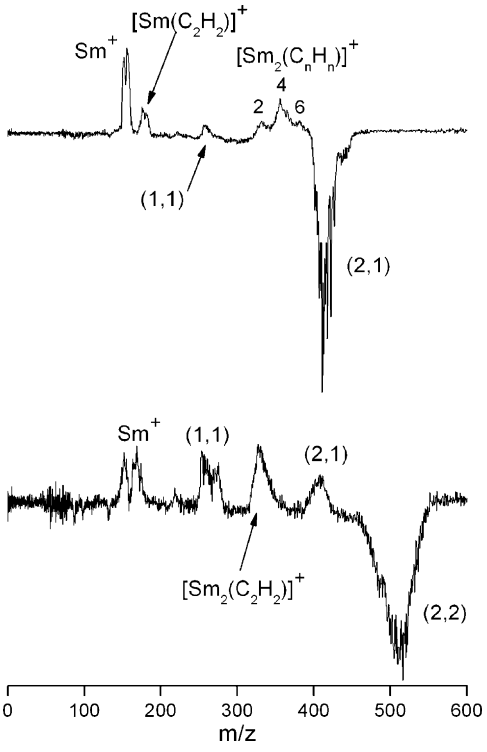

Fig. 3. The top frame shows the photodissociation spectra of $[Sm_2(COT)]^+$ at 355 nm and at high laser power. The lower frame shows the photodissociation of $[Sm_2(COT)_2]^+$ at 355 nm.

To explore these systems beyond the mass spectral abundances, which can clearly vary with conditions, we use mass-selected photodissociation spectroscopy. The top frame of Fig. 2 shows the photodissociation of the $[Sm(COT)]^+$ complex. The parent ion is shown as a negative peak indicating depletion due to fragmentation, while the fragments appear positive. The most prominent fragment is the metal ion itself. When clusters such as these dissociate, it is generally true that the fragment with the lower ionization potential (IP) is observed as an ion, while the fragment with the higher IP is lost as a neutral and is not detected. Examples of so-called "charge transfer dissociation" have been found for metal–benzene complexes [4,5], but this is relatively uncommon for other systems. The IP of samarium is 5.64 eV, whereas that for COT is 8.0 eV [52]. Therefore, production of the metal ion in this case is understandable. Furthermore, the clean elimination of the COT ligand indicates that $[Sm(COT)]^+$ is a "simple" ion-molecule complex without any ligand decomposition or rearrangement.

The lower frame of Fig. 2 shows the photodissociation of the $[Sm(COT)_2]^+$ cluster. The primary product is $[Sm(COT)]^+$, formed by cleanly eliminating a neutral COT molecule. There is also a small amount of the Sm^+ ion fragment. This is more than likely produced by further fragmentation of the $[Sm(COT)]^+$ fragment. Because $[Sm(COT)]^+$ appears as an ionic fragment, it almost certainly has an IP that is lower than that of COT. Additionally, since the COT ligands should experience a greater attraction for the metal ion than for each other, we would expect that this complex exists as a sandwich structure. The fragmentation pattern is consistent with this, indicating the "peeling off" of ligand layers.

In the top frame of Fig. 3, the fragmentation of $[Sm_2(COT)]^+$ is shown. The fragmentation pattern here is markedly different from that in Fig. 2. Instead of simple ligand elimination, fragment ions are detected corresponding to ligand decomposition. The dissociation shows a loss of C_2H_2 units, resulting in a prominent $[Sm_2(C_4H_4)]^+$ peak along with less intense $[Sm_2(C_6H_6)]^+$ and $[Sm_2(C_2H_2)]^+$ peaks. The mass spectrum of COT alone [52], not shown here, shows that COT dissociates into $C_nH_n^+$ units with the most prominent fragment being $C_6H_6^+$. The presence of the two samarium atoms seems to cause COT to fragment in a similar way through the loss of one C_2H_2 unit at a time. In other fragment ions, a small amount of $[Sm(COT)]^+$ is detected, which corresponds to elimination of a neutral Sm atom. There are also peaks corresponding to Sm^+ and $[Sm(C_2H_2)]^+$, which could come sequentially by fragmentation of the Sm_2 ions already mentioned or directly through parallel channels. Sm^+, for example, could come from elimination of this metal cation from the parent ion together with a corresponding neutral Sm(COT) unit. Unfortunately, we are not able to distinguish between these alternatives. $Sm_2(COT)$ has been observed in solution phase chemistry to be an inverted sandwich with samarium atoms on either side of the COT molecule [50]. Separated metals make sense because of the charge transfer and ionic bonding in these systems, which would tend to produce positive metal atoms that would avoid each other. The fragments observed in this spectrum could come from such an inverted sandwich structure, but other alternatives cannot be ruled out. It is clear, however, that

fragmentation is much more extensive in these complexes when two metal atoms are present. Because there was little evidence for such fragmentation in the ions that grew in the source, this fragmentation appears to be photoinduced, i.e., caused by the laser excitation, as opposed to resulting from ground state metal insertion chemistry.

It is interesting to consider the possible structures of fragment ions seen here, such as the $[Sm_2(C_4H_4)]^+$ species. This complex could exist in a open chain structure with samarium atoms attached to vicinal double bonds, as shown below. If this is the case, it would provide a

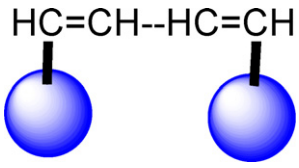

convenient explanation for the $[Sm(C_2H_2)]^+$ ion, which could come from further fragmentation of such an open structure. Another fascinating possibility is that $[Sm_2(C_4H_4)]^+$ is a four membered ring (cyclobutadiene) sandwiched by two metal atoms. Although cyclobutadiene itself is highly strained, a number of metal–cyclobutadiene complexes are known to be quite stable [53]. In such a ring structure, C_4H_4 has four π electrons, and charge donation from the metal would allow a more stable near-aromatic configuration to be achieved for this ligand.

The photodissociation mass spectrum for the $[Sm_2(COT)_2]^+$ cluster is shown in the bottom frame of Fig. 3. Lower signal intensity, decreased resolution at this higher mass, and the several isotopes from the two samarium atoms make the peaks look broad and noisy. The heaviest photofragment observed corresponds to the loss of an entire COT ligand yielding the $[Sm_2(COT)]^+$ cluster. From here, one might expect a similar fragmentation pattern to that seen above for $[Sm_2(COT)]^+$. Some of the same fragments are indeed seen, but there is a much more prominent $[Sm(COT)]^+$ peak and $[Sm_2(C_2H_2)]^+$ is now more intense than the $[Sm_2(C_4H_4)]^+$ seen above. The $[Sm(COT)]^+$ ion could result from elimination of a stable neutral Sm(COT) complex from the parent ion, in the same way that the Sm^+ ion was produced from the $[Sm_2(COT)]^+$ parent. As noted above, neutral Sm(COT) could be stable in a Sm^{2+},COT^{2-} configuration, with Sm in the 2+ oxidation state. The neutral and ionic 1,1 fragments are consistent with a structure for the parent cluster that has alternating metal and ligand stacking, as has been suggested previously for these systems.

The top frame of Fig. 4 shows the photodissociation spectrum of $[Dy(COT)]^+$. The main fragment is Dy^+. The IP of dysprosium (5.93 eV) is lower than that of COT, and as discussed above, one would expect the lower IP species to appear as the charged fragment. Additionally, there are peaks corresponding to $[Dy(C_nH_n)]^+$ ($n = 2, 4, 5, 6$) in this spectrum with $[Dy(C_5H_5)]^+$ being by far the most prominent. The $[Dy(C_5H_5)]^+$ ion was also seen in the mass spectrum produced by the cluster source following photoionization. Because this fragmentation channel requires the loss of the relatively unfavorable neutral C_3H_3, we can assume that $[Dy(C_5H_5)]^+$ is itself quite stable. It is well known that C_5H_5, which has five π electrons, can

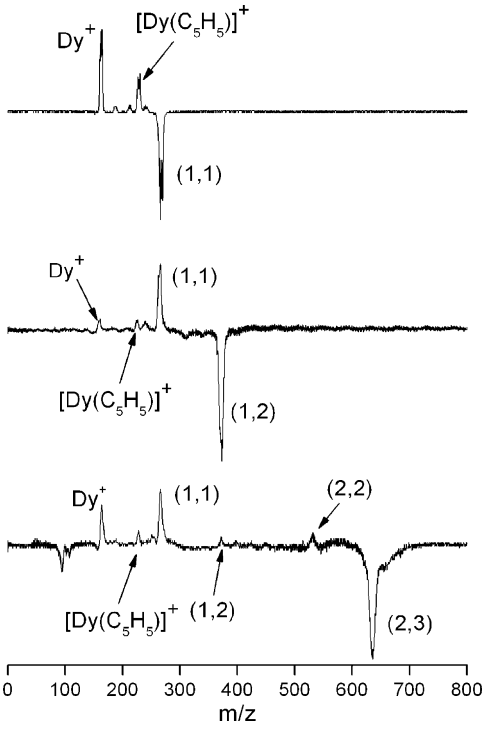

Fig. 4. Photodissociation spectra of $[Dy(COT)]^+$ at 355 nm (top frame), $[Dy(COT)_2]^+$ at 355 nm (middle frame) and $[Dy_2(COT)_3]^+$ at 355 nm (bottom frame).

become aromatic as the cyclopentadienyl anion when it receives charge donation via metal complexation. If we assume that this occurs here, $a+2$ metal oxidation state would produce a stable $[Dy^{2+},C_5H_5{}^-]^+$ species with a net +1 charge. Like most of the lanthanides, dysprosium usually prefers the +3 oxidation state, although it does form some complexes in the +2 oxidation state such as DyI_2 and $DyCl_2$ [54]. Apparently, the +2 oxidation state is somewhat favorable in the present $[Dy(C_5H_5)]^+$ system.

The middle and lower frames of Fig. 4 show the photodissociation of $[Dy(COT)_2]^+$ and $[Dy_2(COT)_3]^+$, respectively. The fragmentation of $[Dy(COT)_2]^+$ shows first the loss of an intact COT molecule and then the loss of the second intact COT molecule leaving only Dy^+. This pattern is what would be expected if $[Dy(COT)_2]^+$ exists in a sandwich formation. There is also a small amount of $[Dy(C_5H_5)]^+$ and $[Dy(C_6H_6)]^+$ present in this spectrum as seen above for the $[Dy(COT)]^+$. The lower frame of Fig. 4 shows the fragmentation of $[Dy_2(COT)_3]^+$, the largest cluster that was photodissociated and one of the more prominent clusters in the mass spectrum. The highest mass fragment is that of $[Dy_2(COT)_2]^+$ which results from elimination of an intact COT molecule from the parent ion. The next highest mass fragment is $[Dy(COT)_2]^+$, which is present in only a small amount. This could result from sequential fragmentation of the 2,2 species by the loss of a dysprosium atom, or directly from the parent ion by elimination of a [Dy(COT)] neutral. Either of these channels makes sense for fragmentation of a parent ion with a sandwich structure. This pattern is apparently continued, as the next prominent fragment is $[Dy(COT)]^+$. Again, this could result from a sequential process by the loss of another COT from the 1,2 species, or by the loss of neutral $[Dy(COT)_2]$

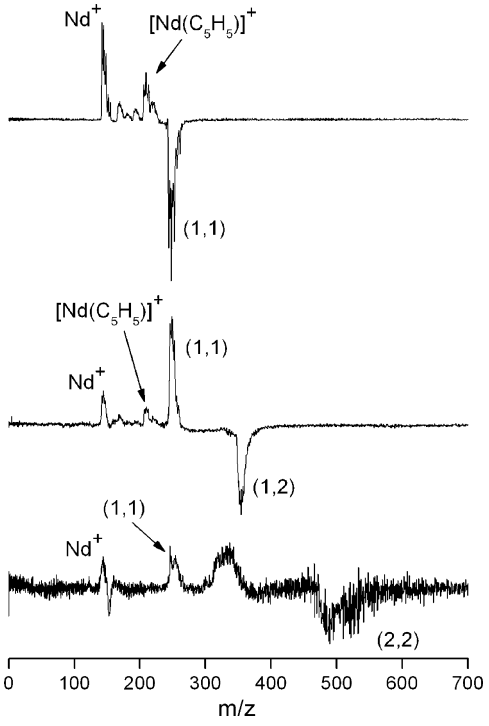

Fig. 5. Photodissociation spectra of $[Nd(COT)]^+$ at 355 nm and high laser power (top frame), $[Nd(COT)_2]^+$ at 355 nm and high laser power (middle frame), and $[Nd_2(COT)_2]^+$ at 355 nm (bottom frame).

directly from the parent ion. The Dy^+ and $[Dy(C_5H_5)]^+$ ions are present in small amounts, and these were also noted above. In all of these processes, there is no evidence for the loss of metal dimer or for the production of a $[Dy_2(COT)]^+$ fragment. Therefore, the simplest structure consistent with the fragmentation pattern for the 2,3 species is a double-decker sandwich, which has been suggested previously for many of these systems.

The top frame of Fig. 5 shows the photodissociation spectra of $Nd^+(COT)$. The main fragmentation peak is Nd^+, which results from a loss of neutral COT. Again, one would expect to see the fragment of the species with the lowest IP. The IP of neodymium is 5.525 eV and COT's IP is 8.0 eV. Therefore, as expected, COT is lost as a neutral molecule and Nd^+ is seen as a fragment peak. Additionally, as with dysprosium, there are peaks corresponding to $[Nd(C_nH_n)]^+$ ($n = 2$–6) with $[Nd(C_5H_5)]^+$ again being the most prominent. The middle frame of Fig. 5 shows the photodissociation of $[Nd(COT)_2]^+$. This fragmentation is exactly the same as that of the $[Dy(COT)_2]^+$ cluster. The two COT ligands are sequentially lost leaving the Nd^+ fragment. This pattern is what would be expected if $[Nd(COT)_2]^+$ exists in a sandwich structure. Also present in this spectrum is a peak corresponding to $[Nd(C_5H_5)]^+$ with smaller peaks corresponding to $[Nd(C_6H_6)]^+$ and $[Nd(C_2H_2)]^+$ as in the spectra for $[Nd(COT)]^+$.

In the bottom frame of Fig. 5 is the photodissociation of $Nd_2{}^+(COT)_2$. The photodissociation efficiency for this system was quite small, producing very poor signal levels, as shown. Nevertheless, some fragments can be identified. In this lower mass region of this spectrum, there are $[Nd(COT)]^+$ and Nd^+ fragment ions, which can come from several channels already mentioned. However, there is also a strong, broad feature near 300–350 amu. This signal lies mostly below the mass of the 1,2 complex, which is indicated as the depletion peak in the middle frame of the figure, and lies near mass 352. Unfortunately, several possible fragment ions could produce signal in this mass region. $[Nd(COT)(C_5H_5)]^+$ would be centered about 313 amu, $[Nd(COT)(C_6H_6)]^+$ would occur near 326 amu, and $[Nd_2(C_4H_4)]^+$ would occur near 340 amu. The benzene ion is perhaps not so likely, as no other benzene ion fragments were detected throughout this study. The $[Nd_2(C_4H_4)]^+$ ion would have a broader isotope distribution from two metals. However, because the overall dissociation signal is weak, and almost any of these ions could produce a broad peak from a slow (metastable) dissociation process. It is therefore not possible to determine which fragments are seen here.

In the transition metal–COT study performed previously by our group, many M^+(benzene) fragment ions were produced by ligand decomposition as the most abundant fragments [41]. This was understandable because of the inherent stability of benzene and because COT itself fragments efficiently to produce benzene by eliminating acetylene. However, no significant amounts of metal–benzene complexes are seen here as fragments. Instead, we see mostly the simple elimination of COT or metal–COT fragments, and when ligand decomposition occurs, there is formation of species such as $[M_n(C_4H_4)]^+$ and $[M_n(C_5H_5)]^+$, where the ligand, like COT, is not aromatic. In the previous work on transition metals, photodissociation of $[V(COT)]^+$ and $[Fe(COT)]^+$ also produced the $[M(C_5H_5)]^+$ ion seen here. The stability of these vanadium and iron fragments was explained by ionic interactions as well as by the 18 electron rule. However, the 18 electron rule does not explain the lanthanide metal complexes produced here, as all of the prominent species have much fewer valence electrons than this. Additionally, the 4d shell is filled for these metals and the 4f orbitals are deeply buried in the atomic core, leaving little overlap with ligand orbitals. Covalent interactions are therefore not efficient. Consistent with this, the only complexes produced here by the source or by fragmentation processes are those with ligands that gain stability by accepting charge. Therefore, the interactions seen here are predominately ionic. Previous studies [44–49] have shown that lanthanide complexes bond very differently than the corresponding transition metal or actinide metal complexes, and favor such ionic interactions.

4. Conclusion

Lanthanide metal complexes of samarium, dysprosium, and neodymium with COT were produced by laser vaporization and studied by fixed frequency ultraviolet laser multiphoton photodissociation. The mass spectral data shows that the complexes are formed by metal atoms, but not clusters of atoms, attaching to COT molecules. Samarium–COT clusters were found to favor 1:1 metal–ligand stoichiometries rather than the $(n,\ n+1)$ pattern seen previously for other lanthanide

metal–COT complexes. Photodissociation of samarium–COT complexes with only one metal atom present exhibited simple elimination of ligands, but those with two metal atoms dissociated via various ligand decomposition channels. A similar trend was seen for neodymium complexes, where ligand decomposition was more efficient in the two-metal complexes. Both dysprosium and neodymium systems produce a prominent $[M(C_5H_5)]^+$ fragment, but samarium does not produce this species.

Taken as a whole, these photodissociation studies confirm some of our expectations about these metal–COT systems, but they also provide unexpected new results. Based on stoichiometries, the previous mass spectrometry of Kaya and coworkers was able to suggest that a number of $M_n(COT)_m$ complexes had multiple-decker sandwich structures. Our conditions do not produce clusters as large as those seen by Kaya, but in the lower masses we see similar stoichiometries. Likewise, those systems that are large enough seem to produce sandwiches or multiple-decker sandwiches. The evidence for this is fragmentation patterns consistent with alternating losses of ligand, then metal, then ligand, etc. The tendency for this is greater for Nd and Dy than it is for Sm. Nd and Dy also have a known tendency to favor the 3+ oxidation state which tends to balance the charge exchange in these systems, and this probably explains this trend. Surprising results from this study include the new decomposition products seen, such as $[Sm_2(C_4H_4)]^+$ and the $[M(C_5H_5)]^+$ ion seen for both Dy and Nd. As noted, the C_4H_4 moiety could represent a cyclobutadiene species, but other structures are also possible for this ligand. A metal in a 2+ state would be expected to be favorable to produce the $[M(C_5H_5)]^+$ species. However, the metal expected to do this most readily (Sm) does not do it at all, and instead the metals that usually have the 3+ oxidation state (Nd, Dy) both form this complex. These various structural questions should be investigated further with theory and perhaps infrared spectroscopy on these systems.

Acknowledgment

We are grateful for support from the U.S. Department of Energy through grant no. DE-FG02-96ER14658.

References

[1] N.J. Long, Metallocenes, Blackwell Sciences, Ltd., Oxford, 1998.
[2] T.J. Kealy, P.L. Paulson, Nature 168 (1951) 1039.
[3] E.O. Fischer, W. Hafner, Z. Naturforsch. 10B (1955) 665.
[4] K.F. Willey, P.Y. Cheng, M.B. Bishop, M.A. Duncan, J. Am. Chem. Soc. 113 (1991) 4721.
[5] K.F. Willey, C.S. Yeh, D.L. Robbins, M.A. Duncan, J. Phys. Chem. 96 (1992) 9106.
[6] T.D. Jaeger, M.A. Duncan, Int. J. Mass Spectrom. 241 (2005) 165.
[7] E.D. Pillai, K.S. Molek, M.A. Duncan, Chem. Phys. Lett. 405 (2005) 247.
[8] K. Hoshino, T. Kurikawa, H. Takeda, A. Nakajima, K. Kaya, J. Phys. Chem. 99 (1995) 3053.
[9] K. Judai, M. Hirano, H. Kawamata, S. Yabushita, A. Nakajima, K. Kaya, Chem. Phys. Lett. 270 (1997) 23.
[10] A. Nakajima, K. Kaya, J. Phys. Chem. A 104 (2000) 176.
[11] T.P. Martin, N. Malinowski, U. Zimmermann, U. Naeher, H. Schaber, J. Chem. Phys. 99 (1993) 4210.
[12] U. Zimmermann, N. Malinowski, U. Naeher, S. Frank, T.P. Martin, Phys. Rev. Lett. 72 (1994) 3542.
[13] F. Tast, N. Malinowski, S. Frank, M. Heinebrodt, I.M.L. Billas, T.P. Martin, Phys. Rev. Lett. 77 (1996) 3529.
[14] F. Tast, N. Malinowski, S. Frank, M. Heinebrodt, I.M.L. Billas, T.P. Martin, Z. Phys. D: At. Mol. Clust. 40 (1997) 351.
[15] W. Branz, I.M.L. Billas, N. Malinowski, F. Tast, M. Heinebrodt, T.P. Martin, J. Chem. Phys. 109 (1998) 3425.
[16] Y. Basir, S.L. Anderson, Chem. Phys. Lett. 243 (1995) 45.
[17] M. Welling, R.I. Thompson, H. Walther, Chem. Phys. Lett. 253 (1996) 37.
[18] A. Nakajima, S. Nagao, H. Takeda, T. Kurikawa, K. Kaya, J. Chem. Phys. 107 (1997) 6491.
[19] T. Kurikawa, S. Nagao, K. Miyajima, A. Nakajima, K. Kaya, J. Phys. Chem. A 102 (1998) 1743.
[20] S. Nagao, T. Kurikawa, K. Miyajima, A. Nakajima, K. Kaya, J. Phys. Chem. A 102 (1998) 4495.
[21] S. Nagao, Y. Negishi, A. Kato, Y. Nakamura, A. Nakajima, K. Kaya, J. Phys. Chem. A 103 (1999) 8909.
[22] J. Suzumura, S. Hosoya, S. Nagao, M. Mitsui, A. Nakajima, J. Chem. Phys. 121 (2004) 2649.
[23] J.E. Reddic, J.C. Robinson, M.A. Duncan, Chem. Phys. Lett. 279 (1997) 203.
[24] J.W. Buchanan, G.A. Grieves, J.E. Reddic, M.A. Duncan, Int. J. Mass Spectrom. 182/183 (1999) 323.
[25] G.A. Grieves, J.W. Buchanan, J.E. Reddic, M.A. Duncan, Int. J. Mass Spectrom. 204 (2001) 223.
[26] B.P. Pozniak, R.C. Dunbar, J. Am. Chem. Soc. 119 (1997) 10439.
[27] J.W. Buchanan, J.E. Reddic, G.A. Grieves, M.A. Duncan, J. Phys. Chem. A 102 (1998) 6390.
[28] J.W. Buchanan, G.A. Grieves, N.D. Flynn, M.A. Duncan, Int. J. Mass Spectrom. 185-187 (1999) 617.
[29] N.R. Foster, G.A. Grieves, J.W. Buchanan, N.D. Flynn, M.A. Duncan, J. Phys. Chem. A 104 (2000) 11055.
[30] M.A. Duncan, A.M. Knight, Y. Negishi, S. Nagao, K. Judai, A. Nakajima, K. Kaya, J. Phys. Chem. A 105 (2001) 10093.
[31] T.M. Ayers, B.C. Westlake, M.A. Duncan, J. Phys. Chem. A 108 (2004) 9805.
[32] T.M. Ayers, B.C. Westlake, D.V. Preda, L.T. Scott, M.A. Duncan, Organometallics 24 (2005) 4573.
[33] A. Klotz, P. Marty, P. Boissel, D. de Caro, G. Serra, J. Mascetti, P. de Parseval, J. Derouault, J.P. Daudey, B. Chaudret, Planet. Space Sci. 44 (1996) 957.
[34] P. Marty, P. de Parseval, A. Klotz, b. Chaudret, G. Serra, P. Boissel, Chem. Phys. Lett. 256 (1996) 669.
[35] P. Marty, P. de Parseval, A. Klotz, G. Serra, P. Boissel, Astron. Astrophys. 316 (1996) 270.
[36] T. Kurikawa, Y. Negishi, F. Hayakawa, S. Nagao, K. Miyajima, A. Nakajima, K. Kaya, J. Am. Chem. Soc. 120 (1998) 11766.
[37] N. Hosoya, R. Takegami, J. Suzumura, K. Yada, K. Koyasu, K. Miyajima, M. Mitsui, M.B. Knickelbein, S. Yabushita, A. Nakajima, J. Phys. Chem. A 109 (2005) 9.
[38] K. Miyajima, M.B. Knickelbein, A. Nakajima, Polyhedron 24 (2005) 2341.
[39] T. Kurikawa, Y. Negishi, F. Hayakawa, S. Nagao, K. Miyajima, A. Nakajima, K. Kaya, Eur. Phys. J. D 9 (1999) 283.
[40] K. Miyajima, T. Kurikawa, M. Hashimoto, A. Nakajima, K. Kaya, Chem. Phys. Lett. 306 (1999) 256.
[41] T.D. Jaeger, M.A. Duncan, J. Phys. Chem. A 108 (2004) 11296.
[42] S. Nagao, A. Kato, A. Nakajima, K. Kaya, J. Am. Chem. Soc. 122 (2000) 4221.
[43] A. Streitwieser, U. Muller-Westerhoff, J. Am. Chem. Soc. 90 (1968) 7364.
[44] K.O. Hodgson, K.N. Raymond, Inorg. Chem. 11 (1972) 3030.
[45] A. Streitwieser, U. Muller-Westerhoff, G. Sonnichsen, F. Mares, D.G. Morell, K.O. Hodgson, C.A. Harmon, J. Am. Chem. Soc. 95 (1973) 8644.
[46] K.O. Hodgson, F. Mares, D.F. Starks, A. Streitwieser, J. Am. Chem. Soc. 95 (1973) 8650.

[47] R.A. Anderson, C.J. Bonsella, C.J. Burns, J.C. Green, D. Hohl, J. Rosch, J. Chem. Soc., Chem. Commun. (1986) 405.
[48] L.J. Nugent, P.G. Laubereau, G.K. Werner, K.L. Vander Sluis, J. Organomet. Chem. 27 (1971) 365.
[49] K.N. Raymond, C.W. Eigenbrot, Acc. Chem. Res. 13 (1980) 276.
[50] F.T. Edelmann, New J. Chem. 19 (1995) 535.
[51] P. Poremba, F.T. Edelmann, J. Organomet. Chem. 553 (1998) 393.
[52] S.G. Lias, in: P.J. Linstrom, W.G. Mallard (Eds.), NIST Chemistry Webbook, Nist Standard Reference Database Number 69, National Institute of Standards and Technology, Gaithersburg, MD, 2005.
[53] A. Efraty, Chem. Rev. 77 (1977) 691.
[54] F.A. Cotton, G. Wilkinson, Advanced Inorganic Chemistry, Wiley-Interscience, New York, 1972.